

Article

Irradiation Induces Tuft Cell Hyperplasia and Myenteric Neuronal Loss in the Absence of Dietary Fiber in a Mouse Model of Pelvic Radiotherapy

Ulrikke Voss ^{1,*}, Dilip Kumar Malipatlolla ², Piyush Patel ^{2,3}, Sravani Devarakonda ², Fei Sjöberg ^{2,3}, Rita Grandér ², Ana Rascón ⁴, Margareta Nyman ⁴, Gunnar Steineck ² and Cecilia Bull ²

¹ Department of Clinical Sciences, Lund University, 221 00 Lund, Sweden

² Division of Clinical Cancer Epidemiology, Department of Oncology, Institute of Clinical Sciences, Sahlgrenska Academy, University of Gothenburg, 413 90 Gothenburg, Sweden; dilip.kumar.malipatlolla@gu.se (D.K.M.); piyush.patel@gu.se (P.P.); sravani.devarakonda@gu.se (S.D.); fei.sjoberg@microbio.gu.se (F.S.); rita.grander@neuro.gu.se (R.G.); gunnar.steineck@oncology.gu.se (G.S.); cecilia.bull@gu.se (C.B.)

³ Department of Infectious Diseases, Institute of Biomedicine, University of Gothenburg, 413 90 Gothenburg, Sweden

⁴ Department of Food Technology, Engineering and Nutrition, Lund University, 221 00 Lund, Sweden; ana.rascon@glucanova.com (A.R.); margareta.nyman@food.lth.se (M.N.)

* Correspondence: ulrikke.voss@med.lu.se



Citation: Voss, U.; Malipatlolla, D.K.; Patel, P.; Devarakonda, S.; Sjöberg, F.; Grandér, R.; Rascón, A.; Nyman, M.; Steineck, G.; Bull, C. Irradiation Induces Tuft Cell Hyperplasia and Myenteric Neuronal Loss in the Absence of Dietary Fiber in a Mouse Model of Pelvic Radiotherapy. *Gastroenterol. Insights* **2022**, *13*, 87–102. <https://doi.org/10.3390/gastroent13010010>

Academic Editor: Piotr Ceranowicz

Received: 31 January 2022

Accepted: 17 February 2022

Published: 22 February 2022

Publisher's Note: MDPI stays neutral with regard to jurisdictional claims in published maps and institutional affiliations.



Copyright: © 2022 by the authors. Licensee MDPI, Basel, Switzerland. This article is an open access article distributed under the terms and conditions of the Creative Commons Attribution (CC BY) license (<https://creativecommons.org/licenses/by/4.0/>).

Abstract: Pelvic radiotherapy is associated with chronic intestinal dysfunction. Dietary approaches, such as fiber enrichment during and after pelvic radiotherapy, have been suggested to prevent or reduce dysfunctions. In the present paper, we aimed to investigate whether a diet rich in fermentable fiber could have a positive effect on radiation-induced intestinal damage, especially focusing on tuft cells and enteric neurons. Male C57BL/6 mice were fed either a purified non-fiber diet or the same purified diet with 5% or 15% oat fiber added, starting two weeks prior to sham-irradiation or irradiation with four fractions of 8 Gray. The animals continued on the diets for 1, 6 or 18 weeks, after which the gross morphology of the colorectum was assessed together with the numbers of enteric neurons, tuft cells and crypt-surface units. The results showed that dietary fiber significantly affected the intestinal morphometrics, both in the short and long-term. The presence of dietary fiber stimulated the re-emergence of crypt-surface unit structures after irradiation. At 18 weeks, the animals fed with the non-fiber diet displayed more myenteric neurons than the animals fed with the dietary fibers, but irradiation resulted in a loss of neurons in the non-fiber fed animals. Irradiation, but not diet, affected the tuft cell numbers, and a significant increase in tuft cells was found 6 and 18 weeks after irradiation. In conclusion, dietary fiber intake has the potential to modify neuronal pathogenesis in the colorectum after irradiation. The long-lasting increase in tuft cells induced by irradiation may reflect an as yet unknown role in the mucosal pathophysiology after pelvic irradiation.

Keywords: tuft cells; irradiation; diet; enteric nervous system; oats; nutrition; fiber; bran; protection

1. Introduction

Cancer-related pelvic radiotherapy is known to cause intestinal complications. Common dysfunctions include fecal urgency, tenesmus, fecal incontinence, diarrhea, mucus leakage and bleeding, all significantly affecting quality of life [1,2]. It has been estimated that approximately 90 percent of pelvic cancer survivors experience permanent changes in their bowel habits, and 50 percent of those with permanent changes perceive that they have a reduced quality of life because of this [3].

Pelvic cancer survivors with intestinal complications are treated with a variety of medical interventions with variable success. Different kinds of dietary advice are common,

but there is no general consensus on their effectiveness. Classically, patients are advised to reduce fiber and fat in their diets after radiation treatment even though there is little evidence-based scientific support for this recommendation [4,5]. Recent studies show favorable outcomes in relation to late pelvic-radiation toxicity in patients given diets rich in fiber [6,7], suggesting that food-based strategies could ameliorate or prevent pelvic-radiation damage. In this respect, dietary fiber interventions are attractive since the material is resistant to human enzymatic digestion, reaching the colon and thus constituting a source of energy and nutrients for the microbiota.

Dietary fiber comprises a large group of structurally diverse compounds whose beneficial impact on intestinal health is believed to be mediated, in part, through their physiochemical properties and effects on microbial activity. Soluble types of fiber are usually degraded to a greater extent by the colon microbiota than insoluble fiber. During this degradation (fermentation), metabolically active compounds can be formed [8], including short-chain fatty acids (SCFAs, mainly acetic, propionic and butyric acids). Depending on the fiber composition, the colon microbiota will produce different amounts and proportions of SCFAs that in turn are associated with diverse physiological effects. Beta-glucans found in barley and oats have been shown to produce especially high amounts of butyric acid, which is an important substrate for colonocytes. Oat bran contains both soluble and fermentable fiber and has been thoroughly evaluated for its potential health benefits [9–11], including immunoregulatory properties [11,12]. The recommended daily intake in adults varies between 18–38 g/day across the globe [13]. These levels are based on amounts needed for laxation and reducing the risk of coronary disease [13]. A low intake of dietary fiber is considered a risk factor for a range of diseases [14], potentially including colorectal cancers [15]. Despite robust data supporting a high intake of dietary fiber the majority of people, including the elderly population, do not reach these recommendations [13,16].

Tuft cells are chemosensory cells present in the intestinal mucosa, decreasing in density from the upper to the lower GI tract [17]. Tuft cells are believed to be critical regulators of the intestinal niche [18] and non-epithelial signals are required for their maintenance and longevity [19]. They play an important role in mucosal maintenance and immunity in response to various stressors [20,21]. For instance, detection of the metabolite succinate by tuft cells in the small intestine triggers type 2 innate immune activity and intestinal remodeling [22]. Genetic ablation of tuft cells impairs the regeneration of the colon following severe injury [19], and tuft cells have also been shown to be involved in the cellular repair response after irradiation [23,24]. They express the SCFA receptor FFAR3 [22], and SCFAs promote the expression of the tuft cell marker Dclk1 in mouse and human enteroid cultures [25]. Tuft cells in the colon have not been characterized in the same detail as in the small intestine but express different markers [26], possibly reflecting the different luminal environment present in the colon compared to the small intestine. Furthermore, tuft cells are found in close proximity to neuronal fibers in the gut [17]. This suggests the potential of a bidirectional communication with the enteric nervous system, which innervates the GI tract and plays an important role in regulation of intestinal function. Like tuft cells, submucosal and myenteric neurons express the FFAR3 receptor and stimulating the receptor may modulate neuronal activity [27,28]. Both tuft cells and myenteric excitatory neurons express choline acetyltransferase (ChAT) [29], and reduced ChAT signaling from enteric neurons appears to provoke an increase in tuft cells to maintain cholinergic homeostasis [30]. It is reasonable to assume that adequate communication is required between these systems for a properly functioning distal colon.

Since fecal urgency and tenesmus are perceived as extremely disabling for pelvic cancer survivors and likely originate from colorectal pathophysiology [2], tuft cells and enteric neurons in the irradiated colorectum are of particular interest. We recently developed a murine model of pelvic radiotherapy employing the same linear accelerators that are used to treat cancer patients [31]. In the model, a total of 32 Gray (Gy) in 4 fractions with a dose rate identical to that given to patients is delivered to a small area encompassing the mouse colorectum. The resulting mucosal pathophysiology is very similar to that

found in irradiated human mucosa. Due to the small radiation field, minimal off-target effects are produced and the animals survive well, maintain a normal weight curve and the pathophysiological processes can be followed over time. Previous findings in the model indicate that colorectal irradiation affects parameters of hippocampal neurogenesis, and that dietary supplementation with a highly fermentable bioprocessed oat bran has the potential to modulate this outcome [32]. The aim of the current study was to investigate whether the model would modify parameters of intestinal health after irradiation, with a particular focus on the population of colorectal tuft cells and enteric neurons.

2. Materials and Methods

2.1. Animals

Male C57BL/6 mice (Charles River Laboratories International, Sulzfeld, Germany.) were used for all the experiments and were approximately nine weeks old at the start of the experiments. All animals were housed five to a cage at a constant temperature (20 °C) and 42% relative humidity. A 12 h dark/light cycle was maintained with lights from 07:00 am to 07:00 pm, and food and water were available ad libitum. All experimental animal procedures were approved by the Gothenburg Committee of the Swedish Animal Welfare Agency (application number 1458-18). The animals were used in accordance with European Community Council Directive (2010/63/EU) and the Swedish Animal Welfare Act (SFS 1988:534), and all applicable international, national and/or institutional guidelines for the care and use of animals were followed.

2.2. Irradiation Procedure

The pelvic radiotherapy model has been described in detail elsewhere [31]. In brief, the radiation was delivered using a linear accelerator (Varian TrueBeam, Varian Medical Systems Inc., Charlottesville, VA, USA) with 6 MV nominal photon energy. The radiation field was $3 \times 3 \text{ cm}^2$, with only the lower quadrant of the field placed over the mice to include approximately 1.5 cm of the distal colon and rectum (colorectum), avoiding the spinal cord and the testicles. A total of 4 fractions of 8 Gy each (32 Gy total) were delivered with 12 h in between. The mouse was anesthetized with isoflurane (MSD Animal Health, Milton Keynes, UK) and placed in a silicone mold, covered with 5 mm thick tissue-equivalent bolus material to obtain a homogeneous absorbed dose distribution throughout the underlying tissue, and irradiated with 8 Gy at a dose-rate of 5.9 Gy/min (Irradiated; "IR"). The procedure took less than five minutes. Dose variation within the target volume was estimated to be $\pm 5\%$. Sham-irradiated ("S-IR") control animals underwent anesthesia under the linear accelerator, with 12 h between each of the 4 anesthesia sessions, but were not irradiated. The $4 \times 8 \text{ Gy}$ regimen was chosen as it produces a pathophysiology in the C57BL/6 mouse colorectum that is very similar to that found in colorectal biopsies from human irradiated cancer survivors [33].

2.3. Diets

Three different diets were investigated and the detailed composition of each is presented in Table 1a–c. A custom-made fiber-free basal mixture (TD 160816, Envigo Teklad Diets, Madison, WI, USA) was supplemented with either purified corn starch, resulting in an isocaloric fiber-free diet (no fiber; "0Fiber") or two different concentrations of highly fermentable bioprocessed oat bran (prepared according to European patent # EP2996492, Glucanova AB, SE), corresponding to either 15% (high oat; "H-oat") or 5% (low oat; "L-oat") in the final diets. The peak molecular weight of the beta-glucan fraction was $101,000 \pm 11,000$ Daltons. The purified cornstarch (Cargill's C*Gel 03401, Caldic Ingredients Sweden AB, Malmö, Sweden) was added to ensure that all the diets had the same dry matter content and were similar with respect to caloric value. To achieve the same amount of dietary fiber in the two fiber-containing diets (15%, dry-weight basis, dwb), 10% dwb non-fermentable cellulose (microcrystalline cellulose, Avicel[®], IE) was added to the low-oat diet. As a reference, a commercial chow diet based on ground wheat, ground corn,

wheat middlings and corn gluten meal was included and results are presented separately in Supplementary Figures S1 and S2 (Normal Chow; “NC”, TD.2016, Envigo Teklad Diets, Madison, WI, USA). All diets were fed to the animals in a porridge-like consistency.

Table 1. (a) Diet composition, (b) ingredients present in the basal mixture and (c) figurative overview.

(a)			
Diet Composition (%)	High Oat 15% Fiber	Low Oat 15% Fiber	No Fiber ¹ 0% Fiber
Bioprocessed oat bran	28.8	9.6	0
Microcrystalline cellulose	0	10	0
Corn starch	4.7	13.9	33.5
Basal mixture	66.5	66.5	66.5
Total	100	100	100

(b)	
Basal Mixture (g/kg of Total Diet in dwb ¹)	
Casein	133
DL-Methionine	2
Corn starch	250
Maltodextrin	87
Sucrose	106
Olive oil	47
Vitamin mixture	10
Choline bitartrate	2
TBHQ ²	0.01
Mineral mixture	13
Calcium phosphate, dibasic	11
Calcium carbonate	4

(c)	
15%	15%

■ Fiber from bioprocessed oat bran ■ Starch and simple sugars
■ Fiber from microcrystalline cellulose ■ Fat
■ Vitamins and minerals ■ Protein

¹ Dry-weight basis. ² Tertiary butylhydroquinone.

2.4. Experimental Design

For all experiments, animals were fed the diet for 2 weeks prior to undergoing either the sham-irradiation (S-IR) or irradiation (IR) procedure, as described above and continued throughout the experiments. The time points for tissue analysis were chosen based on previous knowledge from our model, with intense crypt degeneration at one week post-irradiation, followed by an active regeneration that is prominent by 6 weeks and then

slowly declines to near-control levels by 18 weeks post-irradiation [33]. For the sake of feasibility, we prioritized the two opposing groups 0Fiber and H-oat, and included them at all three time points. We performed two separate runs for the one-week time-point, where experiment 1 comprised NC, 0Fiber and L-oat, and experiment 2 0Fiber and H-oat. It was not possible to merge the data from the two experiments performed on different occasions without risking introducing unknown variables, thus the two runs are presented separately. The intermediate time point diet at 6 weeks post-irradiation comprised H-oat and 0Fiber, while for the late effects in experiment 4 (18 weeks post-irradiation) we also included 0Fiber, L-oat and NC.

2.5. Tissue Harvesting

Animals were deeply anesthetized with isoflurane (Isoba[®] vet, MSD Animal Health, Milton Keynes, UK). Approximately 7 mm of irradiated or sham-irradiated distal colorectum was excised. The shape of the colorectum was preserved and the sample was prevented from curling during fixation by inserting thin soft silicone tubing (OD 1.19 mm ID 0.64 mm, AgnThos, Stockholm, Sweden) before the excision. The tissue samples were then immediately transferred in freshly prepared methacarn (methanol-Carnoy) and fixed for 24 h, followed by washings in methanol, ethanol, xylene and embedding in paraffin. The silicon tubing was removed prior to paraffin embedding. The tissues were cut perpendicular to the longitudinal axis of the colorectum, generating 4 µm thin circular sections. The sections were then mounted in a serial manner (1:6 series), so that adjacent sections on a slide were collected at least 20 µm apart. This ensured that we did not analyze the same area twice.

2.6. Histology and Immunohistochemistry

Sections were deparaffinized with xylene and rehydrated through a graded series of ethanol. For histological evaluation, slides underwent hematoxylin and eosin (H&E) staining. For immunohistochemical evaluation, the slides were subjected to antigen retrieval by microwaving twice for 8 min, at 650 W, in citric acid buffer (0.01 M, pH 6). After cooling, the slides were washed for 20 min in running tap water, and an additional 10 min in PBS with 0.25% Triton X-100 (PBS-T). Double immunolabeling was performed by overnight incubation in a moist chamber at 4 °C, with a mixture of primary antibodies. Enteric neurons were identified using an antibody against PGP9.5 and tuft cells by using an antibody against the established pan-maker Dclk-1 [34]. While other markers for both neurons and tuft cells exist, these were found to work with the methacarn fixation. Secondary antibodies were mixed and incubated for 1 h at room temperature. For details on primary and secondary antibodies, see Table 2. All the antibodies were diluted in phosphate-buffered saline (PBS) containing 0.25% Triton X-100 and 0.25% BSA (PBS-T-B). Cell nuclei were stained with Hoechst (ThermoFisher Scientific, SE), according to the manufacturer's protocol. Mounting was in PBS:glycerol 1:1.

Table 2. Overview of the primary and secondary antibodies used.

Raised Against	Dilution	Source/RRID
Double-cortin-like kinase –1 (DCLK1)	1:250 GR296884 1:2000 GR313013	Abcam ab37994, RRID:AB_873538
Protein gene product 9.5 (PGP9.5)	1:2000	Ultraclone RA95101, RRID:AB_2313685
Alexa Fluor 594 anti-rabbit IgG	1:1000	Jackson ImmunoResearch Europe Ltd. 711-515-152

The H&E-stained slides were scanned in the brightfield setting, while the slides labeled with immunofluorescence were scanned in the fluorescent setting at 20X using a digital slide scanner (Nanozoomer-2HT, and NDP.view2 software, Hamamatsu, Japan). The quantifications and area measurement were performed on digitally scanned images using

the NDP.view software. For tissues to be included in the analysis of morphology, tissues had to have a clear outline of the tubing, absence of luminal content and lack of tissue stretching or contraction. For tissues to be included in the analysis of neuronal density, a whole muscularis and submucosal circumference had to be present. For tissues to be included in the analysis of tuft cells/crypt-surface unit, no fewer than 6 histological intact crypt-surface units should be present. Due to the stringent criteria prioritizing validity, the final number of animals analyzed was reduced to $n = 3-10$. All cell calculations and measurements were performed manually blinded to treatment.

2.7. Morphology

The gross morphology was assessed by measuring the mucosal area from mucosa muscularis to luminal edge, and the muscularis propria area from mucosa muscularis to the outer edge of longitudinal muscle. The average area in mm^2 was calculated from two whole nonconsecutive circular sections per animal.

2.8. Neuronal Numbers

All myenteric ganglia and submucosal ganglia neurons were quantified in two whole nonconsecutive circular sections per animal, and the average was calculated.

2.9. Tuft Cells and Crypt-Surface Unit Numbers

The number of tuft cells was calculated per histological intact crypt-surface unit. For a crypt-surface unit to be included, a clear morphological structure had to be present. For tuft cells to be included, they had to be situated in a morphologically intact crypt-surface unit and display a fungiform shape. Tuft cells and intact crypt-surface units were calculated from two whole nonconsecutive sections per animal.

2.10. Statistical Analyses

Each experiment was analyzed separately to avoid potential batch differences. The analyses of treatment and diet interactions in intestinal measures of health post radiation were performed by the two-way analysis of variance (ANOVA) followed by Sidak's post hoc analysis of means (GraphPad Prism 8, San Diego, CA, USA). QQ plots were evaluated to check for normality (Supplemental Figure S3). Comparisons were performed using appropriate controls. A confidence level of 0.05 was considered significant. Data are presented as mean \pm SD.

3. Results

3.1. General Observations

All irradiated tissues displayed areas of normal intestinal morphology interspersed with abnormal areas. At all the timepoints post-irradiation, a mucosal lining was present.

At week 1 post-irradiation, large areas with short and dispersed crypts were present. At weeks 6 and 18, areas of short, dispersed as well as swollen, and branched crypts were present after irradiation. The morphometric analyses of the short-term effects (1 week) showed a significant effect of diet (ANOVA, $p < 0.01$) and irradiation (ANOVA, $p < 0.05$) for L-oat and 0Fiber on the mucosal area, as well as an interaction (ANOVA, $p < 0.05$) on the muscularis propria area. Multiple comparisons showed a tendency towards a reduced mucosal area in the 0Fiber group compared with L-oat ($p = 0.06$) also present in the irradiated groups ($p = 0.05$). Further, animals fed L-oat had a significantly increased muscularis propria area compared to 0Fiber ($p = 0.008$) (Figure 1A–D). Morphometric analyses of the intermediate effects (6 weeks) showed a diet effect on mucosal area (ANOVA, $p < 0.05$), but no significant differences were observed in the multiple comparison analyses compared with non-irradiated controls. Neither were the effects of diet or irradiation observed on the muscularis propria area (Figure 1F,G). Analyses at 18 weeks showed a significant effect of diet (ANOVA, $p < 0.05$) and irradiation (ANOVA, $p < 0.01$) on the mucosal area. However, multiple comparisons revealed no significant difference compared

to controls. A significant effect of diet were found in the analyses of the muscularis propria area (ANOVA, $p < 0.05$) and multiple comparisons revealed that animals in the H-oat group had reduced muscularis propria compared to the L-oat group ($p = 0.02$) (Figure 1I,J). In conclusion, morphometric analyses showed that dietary fiber altered, in particular, the area of the muscularis propria, both in the short and long-term. L-oat animals displayed an increased area present at 1, but not at 18 weeks of post-S-IR, and H-oat animals showed a reduced muscularis propria at 18 weeks S-IR. Representative micrographs are presented in Figure 1E–K.

3.2. Myenteric Neurons

The myenteric ganglia are a key in regulating intestinal motility and several models, including high-fat diet and stroke, have been shown to induce loss of neurons in this plexus [35,36]. In the groups used in assessing the short-term effects (1 week), no effect of diet or radiation was found on myenteric neuronal numbers (Figure 2A,C). In the intermediate-term experiment (6 weeks), an interaction was found (ANOVA, $p < 0.05$), and post hoc analyses showed significantly more myenteric neurons in the H-oat group after irradiation compared to the 0Fiber group ($p = 0.002$) (Figure 2E). In the long-term experiment (18 weeks), significant effects of both diet (ANOVA, $p < 0.01$) and radiation (ANOVA, $p < 0.05$) were observed, with more myenteric neurons in the 0Fiber group compared to the L-oat ($p = 0.03$) and H-oat ($p = 0.005$) groups. Interestingly, it was only in the 0Fiber group that irradiation induced the loss of myenteric neurons ($p = 0.03$) (Figure 2G). In conclusion, the continued intake of the 0Fiber, L-oat and H-oat diets modulated myenteric neuronal numbers. At 18 weeks post-S-IR the 0Fiber animals displayed more myenteric neurons compared to L-oat and H-oat S-IR animals. The 0Fiber group was also more susceptible to irradiation-induced neuronal loss.

3.3. Submucosal Neurons

The submucosal ganglia have in several models of intestinal dysfunction shown a resilience to loss and damage [35,36]. The submucosal ganglia play important roles in the regulation of luminal secretions. Diarrhea is a known complication of radiotherapy and the submucosal ganglia deserve further investigation because of this. We were unable to identify any statistically significant effects of diet or irradiation on the number of submucosal neurons at any of the timepoints (Figure 2B,D,F,H). At 18 weeks, there was a tendency towards an effect of diet (ANOVA, $p = 0.07$).

3.4. Tuft Cells

Tuft cells have been shown to play an important role in maintaining the epithelial barrier after irradiation [23]. An effect of diet (ANOVA, $p < 0.05$) was observed on tuft cell numbers at one-week post-irradiation. Multiple comparisons revealed the presence of more tuft cells in L-oat animals after irradiation than in 0Fiber animals after irradiation ($p = 0.02$) (Figure 3A,C). In the intermediate-term experiment (6 weeks), an irradiation effect was observed (ANOVA, $p < 0.0001$), with irradiation inducing a significant increase in tuft cells in both 0Fiber ($p = 0.0009$) and H-oat ($p = 0.02$) (Figure 3F). In the long-term experiment (18 weeks), significant effects of radiation on tuft cell numbers (ANOVA, $p < 0.0001$) was found. Irradiation treatment significantly increased tuft cell numbers in all diets (0Fiber $p = 0.01$, L-oat $p = 0.01$, H-oat $p = 0.0004$) compared to their respective controls (Figure 3I). In conclusion, irradiation treatment induced a long-lasting and significant increase in tuft cells, regardless of diet. The results and representative micrographs are presented in Figure 3E–K.

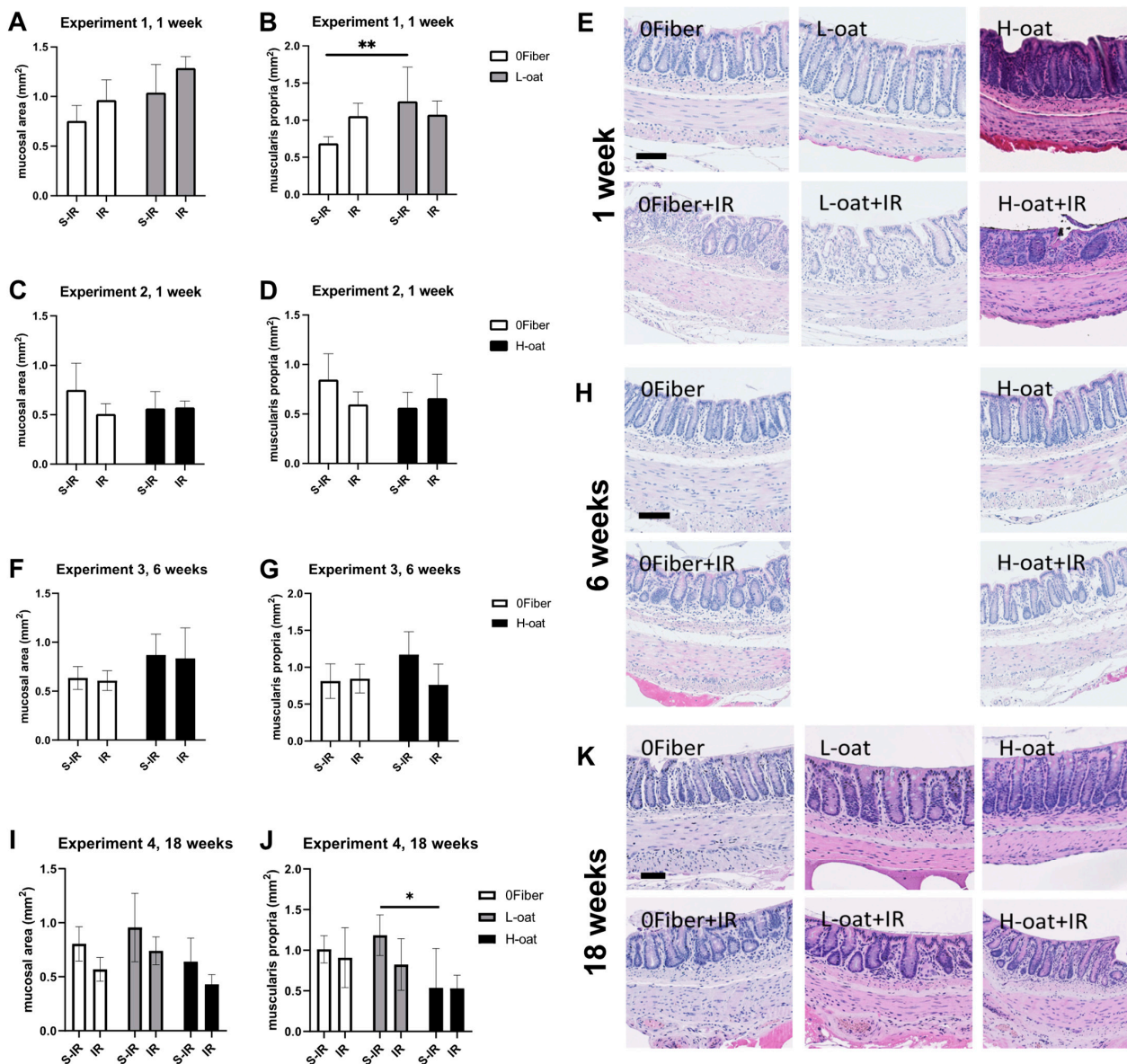


Figure 1. Effects of diet and irradiation on the gross intestinal morphology. (A–E) Morphometric and histological analyses of the mucosal and muscularis propria area after 3 weeks of feeding and 1 week sham-irradiation (S-IR) or irradiation (IR) treatment. (A,B) Experiment 1 showed the L-oat to induce a thickened muscularis propria compared to 0Fiber. (C,D) Experiment 2, no effect of diet or radiation on mucosal (C) or muscularis propria (D) was found. (E) Representative micrographs of colorectum after 1 week of undergoing either S-IR (upper row) and IR (bottom row). Irradiation, regardless of diet, induced disruption of crypt structure. (F,G) Experiment 3, morphometric analyses revealed no effect on mucosal and muscularis propria area after 8 weeks of feeding and 6 weeks, after S-IR or IR treatment. (H) Representative micrographs after 6 weeks of undergoing either S-IR (upper row) or IR (bottom row) treatment. (I,J) Experiment 4, no significant differences between the mucosal areas (I) was observed, but a reduction in the muscularis propria area was observed in H-oat compared to L-oat at 20 weeks of feeding and 18 weeks after undergoing S-IR or IR treatment (J). (K) Representative micrographs after undergoing either S-IR (upper row) or IR (bottom row). At week 6 and week 18 after irradiation, areas of short, dispersed as well as swollen and branched crypts were present and proper crypt structure was re-emerging. S-IR sham-irradiation, IR irradiation, $n = 3-10$, * $p < 0.05$, ** $p < 0.01$. Scale bar represents 50 μm . Note that data are presented as mean \pm SD.

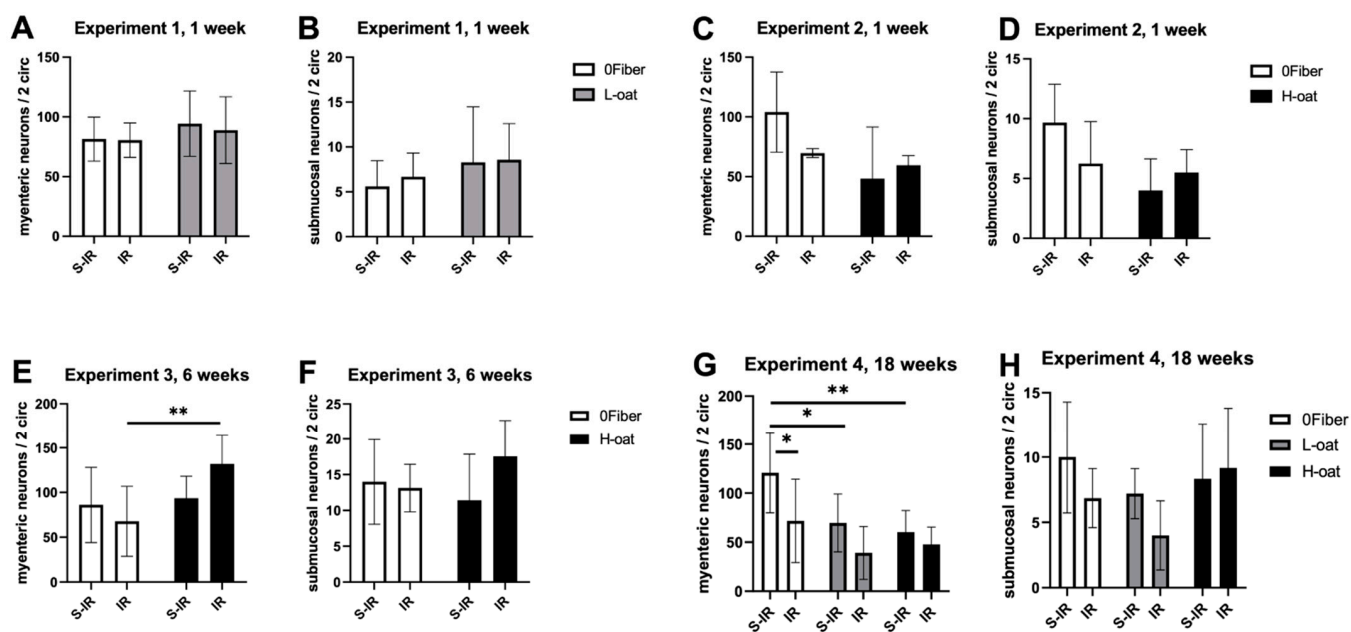


Figure 2. Effect of diet and irradiation on enteric neuronal numbers. (A,B) In experiment 1, the measures of myenteric (A) and submucosal (B) neurons showed no effect of diet or irradiation at 1 week. (C,D) In experiment 2, no effect of diet or irradiation on myenteric (C) and submucosal (D) neuronal numbers was found. (E,F) In experiment 3, more myenteric neurons (E) were observed in the H-oat IR group compared to the 0Fiber IR group. No effects on the submucosal (F) neuronal numbers were observed. (G) In experiment 4, the 0Fiber group displayed more myenteric neurons compared to animals fed L-oat and H-oat. Irradiation significantly reduced the number of myenteric neurons in the 0Fiber IR group but not the L-oat or H-oat group. (H) In experiment 4, there was no effect of diet or irradiation on the submucosal neuronal numbers. S-IR sham-irradiation, IR irradiation, $n = 3-10$, * $p < 0.05$, ** $p < 0.01$. Note that data are presented as mean \pm SD.

3.5. Crypt-Surface Units

The regeneration of the crypt-surface units plays a key role in maintaining intestinal barrier function. At one week, the analysis of histologically intact crypt-surface units per two circumferences showed a significant effect of irradiation (ANOVA, $p < 0.01$), with irradiation significantly reducing the number in both 0Fiber ($p = 0.04$) and L-oat ($p = 0.03$) animals. Additionally, when comparing 0Fiber and H-oat, a significant effect of irradiation was observed (ANOVA, $p < 0.01$), where the number of histologically intact crypt-surface units in H-oat ($p = 0.007$) was lower. Statistical significance was not achieved in the 0Fiber group ($p = 0.06$), potentially reflecting fewer animals reaching our histological inclusion criteria (Figure 3B,D). At 6 weeks, an interaction was observed (ANOVA, $p < 0.05$), and post hoc analysis showed a reduced number of crypt-surface units in the irradiated 0Fiber group compared to the sham-irradiated 0Fiber group (Figure 3G). At 18 weeks, an irradiation effect can still be observed (ANOVA, $p < 0.05$), but multiple comparisons reveal no difference between the irradiated groups and their appropriate controls (Figure 3J). In conclusion, irradiation reduced the number of intact crypt-surface units at 1 week but, at 6 weeks, the H-oat group had potentially regenerated a number of morphological crypt-surface units, since no significant difference was observed. At 18 weeks, all the irradiated diet groups had overall fewer histological crypt-surface units, but the loss was less pronounced since no significant difference in numbers was observed between irradiated and sham-irradiated control animals.

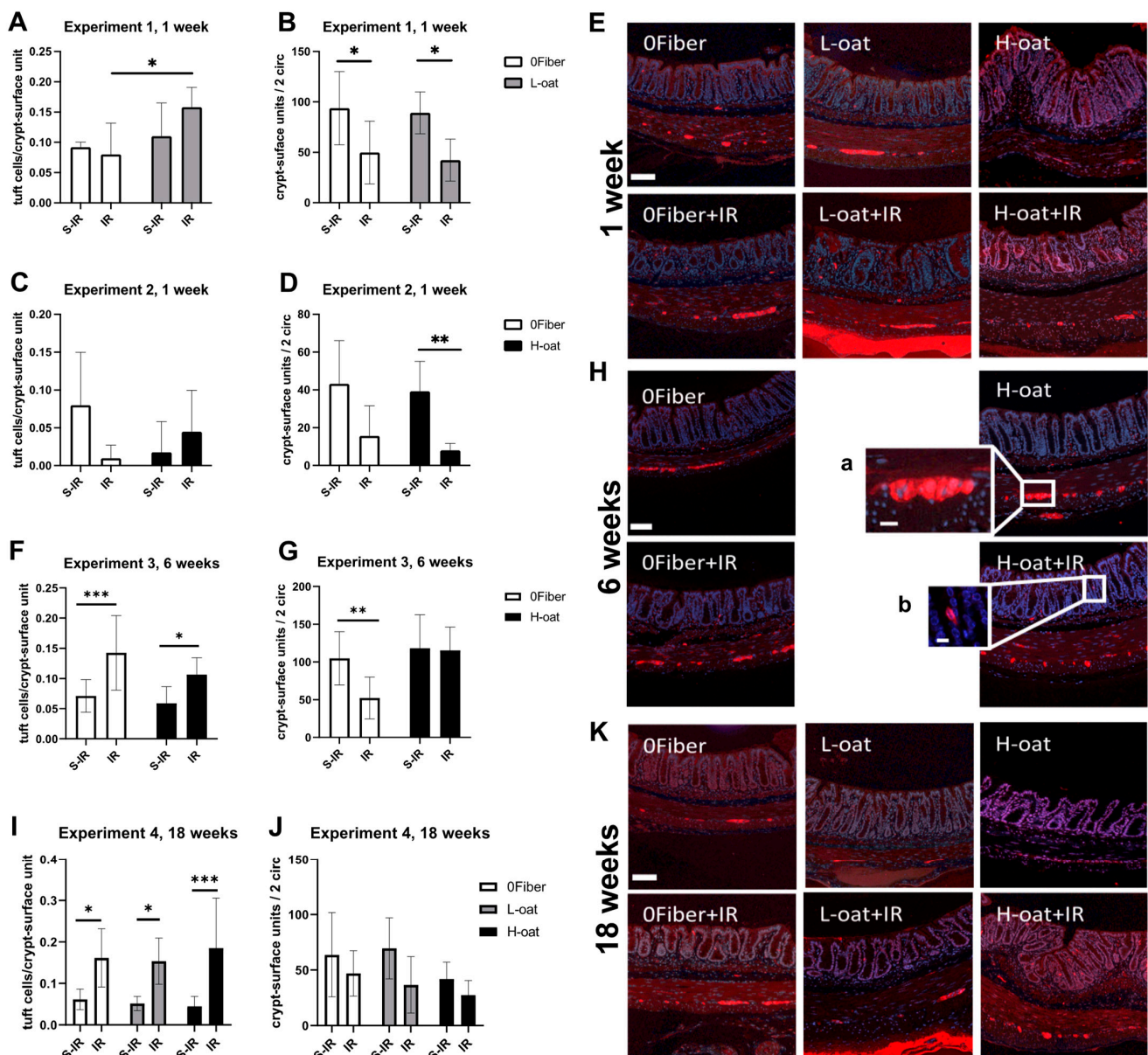


Figure 3. Effect of diet and irradiation on tuft cells and intact crypt-surface units after sham-irradiation (S-IR) or irradiation (IR) treatment. (A–E) Experiment 1, significantly more tuft cells were present in the L-oat irradiation group compared to 0Fiber irradiation group (A). Irradiation significantly decreased the number of intact crypts-surface units (B) regardless of diet after 1 week. (C,D) In experiment 2, no effect of diet or treatment was observed with regard to tuft cell numbers (C), but a significant decrease in the intact crypt-surface unit numbers (D) after irradiation was found in the H-oat group. (E) Representative micrographs of the enteric neurons and tuft cells in colorectum 1 week after S-IR (upper row) or IR (bottom row). (F–H) Experiment 3 showed a radiation-induced increase in tuft cells (F) present at 6 weeks after treatment. A reduced number of crypt-surface units (G) was present in the 0Fiber, but not in the H-oat group. (H) Representative micrographs of enteric neurons and tuft cells after 8 weeks of feeding and 6 weeks after undergoing either S-IR (upper row) or IR (bottom row). Insert (a) myenteric ganglion, (b) tuft cell. (I–K) In experiment 4, a significant increase in tuft cells was found (I) after irradiation, regardless of diet. No significant differences in the treatment was observed in crypt-surface unit numbers (J). (K) Representative micrographs of enteric neurons and tuft cells, 18 weeks after undergoing either S-IR (upper row) or IR (bottom row). S-IR sham-irradiation, IR irradiation, $n = 3-10$, * $p < 0.05$, ** $p < 0.01$, *** $p < 0.001$. Scale bar represents 50 μm , scale bar in inserts represents 20 μm . Note that data are presented as mean \pm SD.

4. Discussion

Oat bran and oat beta-glucans have been shown to increase intestinal transit time, be fermented in the large intestine, and act as a prebiotic and to form specific SCFAs [11,37,38]. They are also known to form especially high amounts of butyric acid [39]. In rodents, fermentation occurs mainly in the cecum, but mixtures of different types of fibers can extend the fermentation into the distal part of the colon [40], providing SCFAs along the entire length of the colon. Since the bioprocessed oat bran used in the present study contains dietary fiber and beta-glucans of different chain lengths, one can assume the production of SCFAs throughout the colon, including the irradiated volume. Interestingly, after 20 weeks of feeding (18 weeks post S-IR), animals consuming the H-oat diet with 15% of fermentable fiber had the smallest muscularis propria area. This long-term effect of the bioprocessed oat bran on the muscularis propria has not previously been shown. Aligning with our results from the L-oat group, it has been shown that 4 weeks of feeding soluble and fermentable fiber pectin induces a thickening of muscularis propria in rats. This was suggested to be due to increased viscosity of luminal content [41]. After 20 weeks of feeding (18 weeks post-S-IR), a lower number of myenteric neurons was observed in the groups fed bioprocessed oat bran compared to the group fed 0Fiber. It is not known if this reflects the different needs for contractive power. Fiber-free diets in rats have been shown to induce changes in contractive response in the distal colon [42]. This was suggested to be partly due to a loss of enteroendocrine cells and reduced amounts of SCFAs in colon [42]. SCFAs were shown to modulate myenteric neuronal chemical coding [28] and colon motility [43]. Oat beta-glucans, present in high amounts in the bioprocessed oat bran, particularly increase the concentration of the SCFA butyrate in the colon of rat at both high and low doses [37]. Butyrate has been associated with an increase in the proportion of excitatory ChAT-positive motor neurons in the colon [28]. Whether or not the reduced muscularis propria area and fewer myenteric neurons observed in this study are correlated to an increase of butyrate in the lumen, leading to an increased proportion of ChAT motor neurons and improved contractile response, can at present only be speculated. It is evident that supplementation with the highly fermentable bioprocessed oat bran alters both the gross intestinal morphology as well as the cell populations in the colorectum in the short and long term.

Pelvic irradiation causes both acute and late-occurring symptoms, such as diarrhea and/or constipation, fecal urgency, tenesmus and fecal leakage [2]. Despite a clear radiation-induced pathophysiology in our model, we did not observe any statistically significant radiation-induced loss of enteric neurons in animals receiving the bioprocessed oat bran. In the 0Fiber group, however, irradiation resulted in a significant loss of myenteric neurons at 18 weeks. It was shown that mucosal and muscular propria innervation is increased in cancer patients 4–7 days after irradiation. However, at 5–6 weeks to several years post-irradiation, a loss of fiber densities is observed [44]. Possibly, the pathophysiology of irradiated mice on a fiber-free diet resembles the human situation more closely, since the fiber intake in humans is far below the recommended level, at least in Western countries [16]. Fiber-deprived diets result in alterations in the neurogenic and myogenic response as well as a reduced presence of enterochromaffin cells [42], and colonization with SCFA-producing bacteria has been shown to play a role in both enterochromaffin and enteric neuronal maturation in mice [45,46]. While our findings suggest that dietary fiber may protect against radiation-induced enteric neuronal loss, it should be noted that neuronal function may still be affected. Radiation may cause changed motility patterns in the intestine without inducing histological alterations [47,48]. Furthermore, radiation has been shown to increase cholinergic and serotonin signaling in the colon [47] and to induce an inflammatory response in the gut, which can affect neurochemical coding and function [49]. It is possible that the increase in tuft cells reflects a compensatory mechanism for altered cholinergic signaling. Tuft cells have been found to sense the loss of cholinergic signaling from neurons and to expand to maintain cholinergic homeostasis [30]. If the tuft cell response is not adequate to restore cholinergic signaling; this might promote dysmotility. Whether the

observed tuft-cell increase is a result of a compensatory mechanism and whether it plays a role in radiation-induced symptoms, such as fecal urgency and tenesmus, remain to be shown. The distal colon is innervated by lumbar splanchnic nerves and sacral pelvic nerves with sensory capacity [50], and an ability to modulate enteric activity, as seen, for example, in altered bowel control in spinal cord-injured patients [51]. In this study, we did not evaluate whether radiation-induced damage to extrinsic nerve innervation was present. However, sacral neuromodulation has been shown to be an effective treatment of radiation-induced fecal incontinence [52], suggesting at least, in part, an altered extrinsic control.

Since radiation targets the DNA, cells that have a quick turnover are initially more affected by radiation, for example, the intestinal epithelial cells. This is observed as barrier breakdown and inflammation in the acute stages of radiation toxicity [53]. Delayed radiation toxicity is not fully understood, but likely involves an imbalance of cellular systems in the gut, including immune, endocrine, neuronal and microbiome systems [53]. The type 2 immune response initiated in response to parasitic infections in the small intestine has a strong tuft cell component [20,54]. This response is mediated through interleukin (IL)-25-induced activation of IL-13 and IL-4 [20,54]. It would be interesting in future studies to determine if irradiation damage initiates a similar innate mechanism in the colon. Previously, we found pro-inflammatory serum cytokines to be upregulated after irradiation at all three timepoints, suggesting a lasting inflammatory activity [55].

Tuft cells in the small intestine have previously been shown to play an important role in the post-irradiation p53-independent response, re-establishing barrier function [23,24]. The radiation-induced breakdown of cells leads to release of bioactive molecules, such as arachidonic acid, from membranes [56], and succinate from mitochondria [57], compounds that tuft cells are known to sense. Furthermore, succinate is shown to induce tuft cell hyperplasia [58]. In a bacterial-induced colitis model, tuft cells were found to support epithelial regeneration via a cyclooxygenase 2 (COX2), arachidonic acid and prostaglandin E2 pathway [59]. Interestingly, COX2 expression is increased after radiation, as are the serum levels of prostaglandin E2 [24]. It is possible that tuft cells sense the signals present in the luminal environment under normal conditions, but upon barrier breakdown and the release of bioactive molecules from the neighboring cells, tuft cells initiate an immune response, which leads to hyperplasia, possibly utilizing the same IL-25 signaling pathway as with infections, since IL-13 is found to be increased in small intestine after irradiation [60]. The increase in tuft cell numbers in this study coincides with possible re-emergence of morphological intact crypt-surface units, perhaps reflecting the importance of tuft cells in the support of the stem cell niche post-irradiation [23,24].

The increase in the tuft cells was evident in our study at 6 and 18 weeks after irradiation, but not at 1 week. The previously observed tuft cell response to radiation was 3.5 days after irradiation [23,24]. The differences may reflect not only the differences in the intestinal segment studied, but also the differences in irradiation protocol. The previous study used a lethal total body irradiation dose of 12 Gy, compared to our non-lethal protocol, with a total dose of 32 Gy delivered in 4 fractions restricted to the distal bowel. Radiation induces oxidative stress, which may not only have short-term but also long-term effects on gene expression through the activation of oxidative stress enzymes [56]. The continued increased presence of tuft cells may reflect a response to a long-lasting change in the oxidative environment leading to continued stress signals. Notably, the prolonged increase in the tuft cells may be a blessing in disguise and possibly be present as a risk factor for future cancer development, since a small and long-lived subpopulation of tuft cells is known to be able to induce adenocarcinoma in certain pro-carcinogenic and injurious situations [19].

This study was performed on young male animals; future studies should include evaluations of both age and gender. To assess colonic functionality, future studies should also include assessments of intestinal motility and barrier permeability.

5. Conclusions

In this study, we found that irradiation led to lasting tuft-cell hyperplasia, regardless of the dietary approach. We speculate that the tuft cell hyperplasia might be a response to a radiation-induced local increase in inflammatory signals, and/or the disruption of nerve cell activity. This could contribute to the underlying pathophysiology driving some of the most disabling symptoms from which irradiated pelvic cancer survivors suffer, including tenesmus and fecal urgency. Future studies to corroborate the findings in pelvic cancer survivors, and efforts to disentangle the role of tuft cells in irradiation-induced intestinal injury, may provide important knowledge in the development of protective or preventative strategies. In addition, our findings add to the growing evidence that dietary intake is an important factor to consider in the strive to maintain, improve, or regain intestinal health across all ages.

Supplementary Materials: The following supporting information can be downloaded at: <https://www.mdpi.com/article/10.3390/gastroent13010010/s1>. Figure S1: Morphometric, neuronal and tuft cell analyses of animals feed normal chow 1 and 18 weeks after sham irradiation or irradiation; Figure S2: Representative micrographs of animals feed normal chow 1 and 18 weeks after sham irradiation or irradiation; Figure S3: QQ plots of normality for experimental analyses.

Author Contributions: C.B., G.S., F.S., A.R. and M.N. designed the experiments; D.K.M., P.P., S.D., R.G., C.B. and F.S. performed the experiments; U.V. designed and performed the analyses; U.V., C.B. and G.S. analyzed the data; U.V., C.B., G.S., A.R. and M.N. contributed to the writing of the manuscript. All authors have read and agreed to the published version of the manuscript.

Funding: U.V. acknowledges grants from the Thure Carlsson's (2017), Albert Pålsson's (2017) and Crafoord (20160754/20181034) foundations, Lund, Sweden. C.B. and G.S. acknowledge grants from the King Gustav V Jubilee Clinic Cancer Foundation (C.B. 2019:216 and G.S. 2020:329), Gothenburg, Sweden, the Swedish Cancer Society Stockholm, Sweden (G.S. CAN 2018/656), the Sahlgrenska Academy Homecoming Award, Gothenburg, Sweden, and the Swedish State under the ALF agreement, Sweden (G.S. 727821).

Institutional Review Board Statement: Animals were used in accordance with the European Community Council Directive (2010/63/EU) and the Swedish Animal Welfare Act (SFS 1988:534), and all applicable international, national and/or institutional guidelines for the care and use of animals were followed.

Informed Consent Statement: Not applicable.

Data Availability Statement: Data is available upon reasonable request.

Acknowledgments: The authors would like to thank Ekblad for suggesting the histological evaluation criteria.

Conflicts of Interest: A.R. is the author of the patent (EP2996492) for oat bran bioprocessing and Chief Scientific Officer at Glucanova AB. All other authors declare no competing interests.

References

1. Andreyev, H.J.N.; Wotherspoon, A.; Denham, J.W.; Hauer-Jensen, M. Defining pelvic-radiation disease for the survivorship era. *Lancet Oncol.* **2010**, *11*, 310–312. [[CrossRef](#)]
2. Steineck, G.; Skokic, V.; Sjöberg, F.; Bull, C.; Alevronta, E.; Dunberger, G.; Bergmark, K.; Wilderäng, U.; Oh, J.H.; Deasy, J.O.; et al. Identifying radiation-induced survivorship syndromes affecting bowel health in a cohort of gynecological cancer survivors. *PLoS ONE* **2017**, *12*, e0171461. [[CrossRef](#)] [[PubMed](#)]
3. Andreyev, H. Gastrointestinal Problems after Pelvic Radiotherapy: The Past, the Present and the Future. *Clin. Oncol.* **2007**, *19*, 790–799. [[CrossRef](#)] [[PubMed](#)]
4. McGough, C.; Baldwin, C.; Frost, G.; Andreyev, H.J.N. Role of nutritional intervention in patients treated with radiotherapy for pelvic malignancy. *Br. J. Cancer* **2004**, *90*, 2278–2287. [[CrossRef](#)] [[PubMed](#)]
5. Stacey, R.; Green, J.T. Radiation-induced small bowel disease: Latest developments and clinical guidance. *Ther. Adv. Chronic Dis.* **2014**, *5*, 15–29. [[CrossRef](#)]

6. Wedlake, L.; Shaw, C.; McNair, H.; Lalji, A.; Mohammed, K.; Klopper, T.; Allan, L.; Tait, D.; Hawkins, M.A.; Somaiah, N.; et al. Randomized controlled trial of dietary fiber for the prevention of radiation-induced gastrointestinal toxicity during pelvic radiotherapy. *Am. J. Clin. Nutr.* **2017**, *106*, 849–857. [[CrossRef](#)]
7. Hedelin, M.; Skokic, V.; Wilderäng, U.; Ahlin, R.; Bull, C.; Sjöberg, F.; Dunberger, G.; Bergmark, K.; Stringer, A.; Steineck, G. Intake of citrus fruits and vegetables and the intensity of defecation urgency syndrome among gynecological cancer survivors. *PLoS ONE* **2019**, *14*, e0208115. [[CrossRef](#)]
8. Jakobsdottir, G.; Nyman, M.; Fåk, F. Designing future prebiotic fiber to target metabolic syndrome. *Nutrition* **2014**, *30*, 497–502. [[CrossRef](#)]
9. El Khoury, D.; Cuda, C.; Luhovyy, B.L.; Anderson, G.H. Beta glucan: Health benefits in obesity and metabolic syndrome. *J Nutr. Metab.* **2012**, *2012*, 851362. [[CrossRef](#)]
10. Ramakers, J.D.; Volman, J.J.; Biorlund, M.; Onning, G.; Mensink, R.P.; Plat, J. Fecal water from ileostomic patients consuming oat beta-glucan enhances immune responses in enterocytes. *Mol. Nutr. Food Res.* **2007**, *51*, 211–220. [[CrossRef](#)]
11. Wilczak, J.; Błaszczyk, K.; Kamola, D.; Gajewska, M.; Harasym, J.P.; Jałosińska, M.; Gudej, S.; Suchecka, D.; Oczkowski, M.; Gromadzka-Ostrowska, J. The effect of low or high molecular weight oat beta-glucans on the inflammatory and oxidative stress status in the colon of rats with LPS-induced enteritis. *Food Funct.* **2015**, *6*, 590–603. [[CrossRef](#)] [[PubMed](#)]
12. Yun, C.-H.; Estrada, A.; Van Kessel, A.; Park, B.-C.; Laarveld, B. β^2 -Glucan, extracted from oat, enhances disease resistance against bacterial and parasitic infections. *FEMS Immunol. Med. Microbiol.* **2003**, *35*, 67–75. [[CrossRef](#)]
13. Jones, J.M. CODEX-aligned dietary fiber definitions help to bridge the fiber gap. *Nutr. J.* **2014**, *13*, 34. [[CrossRef](#)] [[PubMed](#)]
14. Veronese, N.; Solmi, M.; Caruso, M.G.; Giannelli, G.; Osella, A.R.; Evangelou, E.; Maggi, S.; Fontana, L.; Stubbs, B.; Tzoulaki, I. Dietary fiber and health outcomes: An umbrella review of systematic reviews and meta-analyses. *Am. J. Clin. Nutr.* **2018**, *107*, 436–444. [[CrossRef](#)]
15. Hidaka, A.; Harrison, T.A.; Cao, Y.; Sakoda, L.C.; Barfield, R.; Giannakis, M.; Song, M.; Phipps, A.I.; Figueiredo, J.C.; Zaidi, S.H.; et al. Intake of Dietary Fruit, Vegetables, and Fiber and Risk of Colorectal Cancer According to Molecular Subtypes: A Pooled Analysis of 9 Studies. *Cancer Res.* **2020**, *80*, 4578–4590. [[CrossRef](#)]
16. King, D.E.; Mainous, A.; Lambourne, C.A. Trends in Dietary Fiber Intake in the United States, 1999–2008. *J. Acad. Nutr. Diet.* **2012**, *112*, 642–648. [[CrossRef](#)]
17. Cheng, X.; Voss, U.; Ekblad, E. Tuft cells: Distribution and connections with nerves and endocrine cells in mouse intestine. *Exp. Cell Res.* **2018**, *369*, 105–111. [[CrossRef](#)]
18. Middelhoff, M.; Westphalen, C.B.; Hayakawa, Y.; Yan, K.S.; Gershon, M.D.; Wang, T.C.; Quante, M. Dclk1-expressing tuft cells: Critical modulators of the intestinal niche? *Am. J. Physiol. Liver Physiol.* **2017**, *313*, G285–G299. [[CrossRef](#)]
19. Westphalen, C.B.; Asfaha, S.; Hayakawa, Y.; Takemoto, Y.; Lukin, D.J.; Nuber, A.H.; Brandtner, A.; Setlik, W.; Remotti, H.; Muley, A.; et al. Long-lived intestinal tuft cells serve as colon cancer-initiating cells. *J. Clin. Investig.* **2014**, *124*, 1283–1295. [[CrossRef](#)]
20. Gerbe, F.; Sidot, E.; Smyth, D.J.; Ohmoto, M.; Matsumoto, I.; Dardalhon, V.; Cesses, P.; Garnier, L.; Pouzolles, M.; Brulin, B.; et al. Intestinal epithelial tuft cells initiate type 2 mucosal immunity to helminth parasites. *Nature* **2016**, *529*, 226–230. [[CrossRef](#)]
21. Schneider, C.; O’Leary, C.E.; Locksley, R.M. Regulation of immune responses by tuft cells. *Nat. Rev. Immunol.* **2019**, *19*, 584–593. [[CrossRef](#)] [[PubMed](#)]
22. Schneider, C.; O’Leary, C.E.; von Moltke, J.; Liang, H.-E.; Ang, Q.Y.; Turnbaugh, P.J.; Radhakrishnan, S.; Pellizzon, M.; Ma, A.; Locksley, R.M. A Metabolite-Triggered Tuft Cell-ILC2 Circuit Drives Small Intestinal Remodeling. *Cell* **2018**, *174*, 271–284.e14. [[CrossRef](#)] [[PubMed](#)]
23. May, R.; Qu, D.; Weygant, N.; Chandrakesan, P.; Ali, N.; Lightfoot, S.A.; Li, L.; Sureban, S.M.; Houchen, C.W. Brief Report: Dclk1 Deletion in Tuft Cells Results in Impaired Epithelial Repair After Radiation Injury. *Stem Cells* **2013**, *32*, 822–827. [[CrossRef](#)] [[PubMed](#)]
24. Chandrakesan, P.; May, R.; Weygant, N.; Qu, D.; Berry, W.; Sureban, S.; Ali, N.; Rao, C.; Huycke, M.; Bronze, M.S.; et al. Intestinal tuft cells regulate the ATM mediated DNA Damage response via Dclk1 dependent mechanism for crypt restitution following radiation injury. *Sci. Rep.* **2016**, *6*, 37667. [[CrossRef](#)]
25. Pearce, S.C.; Weber, G.J.; Van Sambeek, D.M.; Soares, J.W.; Racicot, K.; Breault, D.T. Intestinal enteroids recapitulate the effects of short-chain fatty acids on the intestinal epithelium. *PLoS ONE* **2020**, *15*, e0230231. [[CrossRef](#)]
26. McKinley, E.T.; Sui, Y.; Al-Kofahi, Y.; Millis, B.A.; Tyska, M.J.; Roland, J.T.; Santamaria-Pang, A.; Ohland, C.L.; Jobin, C.; Franklin, J.L.; et al. Optimized multiplex immunofluorescence single-cell analysis reveals tuft cell heterogeneity. *JCI Insight* **2017**, *2*, e93487. [[CrossRef](#)]
27. Nøhr, M.K.; Pedersen, M.H.; Gille, A.; Egerod, K.L.; Engelstoft, M.S.; Husted, A.S.; Sichlau, R.M.; Grunddal, K.V.; Poulsen, S.S.; Han, S.; et al. GPR41/FFAR3 and GPR43/FFAR2 as cosensors for short-chain fatty acids in enteroendocrine cells vs FFAR3 in enteric neurons and FFAR2 in enteric leukocytes. *Endocrinology* **2013**, *154*, 3552–3564. [[CrossRef](#)]
28. Soret, R.; Chevalier, J.; De Coppet, P.; Poupeau, G.; Derkinderen, P.; Segain, J.P.; Neunlist, M. Short-Chain Fatty Acids Regulate the Enteric Neurons and Control Gastrointestinal Motility in Rats. *Gastroenterology* **2010**, *138*, 1772–1782.e4. [[CrossRef](#)]
29. Hayakawa, Y.; Sakitani, K.; Konishi, M.; Asfaha, S.; Niikura, R.; Tomita, H.; Renz, B.W.; Taylor, Y.; Macchini, M.; Middelhoff, M.; et al. Nerve Growth Factor Promotes Gastric Tumorigenesis through Aberrant Cholinergic Signaling. *Cancer Cell* **2017**, *31*, 21–34. [[CrossRef](#)]

30. Middelhoff, M.; Nienhüser, H.; Valenti, G.; Maurer, H.C.; Hayakawa, Y.; Takahashi, R.; Kim, W.; Jiang, Z.; Malagola, E.; Cuti, K.; et al. Prox1-positive cells monitor and sustain the murine intestinal epithelial cholinergic niche. *Nat. Commun.* **2020**, *11*, 111–114. [[CrossRef](#)]
31. Bull, C.; Malipatlolla, D.; Kalm, M.; Sjöberg, F.; Alevronta, E.; Grandér, R.; Sultanian, P.; Persson, L.; Boström, M.; Eriksson, Y.; et al. A novel mouse model of radiation-induced cancer survivorship diseases of the gut. *Am. J. Physiol. Liver Physiol.* **2017**, *313*, G456–G466. [[CrossRef](#)] [[PubMed](#)]
32. Devarakonda, S.; Malipatlolla, D.K.; Patel, P.; Grandér, R.; Kuhn, H.G.; Steineck, G.; Sjöberg, F.; Rascón, A.; Nyman, M.; Eriksson, Y.; et al. Dietary Fiber and the Hippocampal Neurogenic Niche in a Model of Pelvic Radiotherapy. *Neuroscience* **2021**, *475*, 137–147. [[CrossRef](#)] [[PubMed](#)]
33. Malipatlolla, D.K.; Patel, P.; Sjöberg, F.; Devarakonda, S.; Kalm, M.; Angenete, E.; Lindskog, E.B.; Grandér, R.; Persson, L.; Stringer, A.; et al. Long-term mucosal injury and repair in a murine model of pelvic radiotherapy. *Sci. Rep.* **2019**, *9*, 13803. [[CrossRef](#)] [[PubMed](#)]
34. Gerbe, F.; Brulin, B.; Makrini, L.; Legraverend, C.; Jay, P. DCAMKL-1 Expression Identifies Tuft Cells Rather Than Stem Cells in the Adult Mouse Intestinal Epithelium. *Gastroenterology* **2009**, *137*, 2179–2180. [[CrossRef](#)] [[PubMed](#)]
35. Voss, U.; Sand, E.; Olde, B.; Ekblad, E. Enteric Neuropathy Can Be Induced by High Fat Diet In Vivo and Palmitic Acid Exposure In Vitro. *PLoS ONE* **2013**, *8*, e81413. [[CrossRef](#)] [[PubMed](#)]
36. Cheng, X.; Boza-Serrano, A.; Turesson, M.F.; Deierborg, T.; Ekblad, E.; Voss, U. Galectin-3 causes enteric neuronal loss in mice after left sided permanent middle cerebral artery occlusion, a model of stroke. *Sci. Rep.* **2016**, *6*, 32893. [[CrossRef](#)]
37. Shen, R.L.; Dang, X.Y.; Dong, J.L.; Hu, X.Z. Effects of oat beta-glucan and barley beta-glucan on fecal characteristics, intestinal microflora, and intestinal bacterial metabolites in rats. *J. Agric. Food Chem.* **2012**, *60*, 11301–11308. [[CrossRef](#)]
38. Kristek, A.; Wiese, M.; Heuer, P.; Kosik, O.; Schar, M.Y.; Soykan, G.; Alsharif, S.; Kuhnle, G.G.C.; Walton, G.; Spencer, J.P.E. Oat bran, but not its isolated bioactive beta-glucans or polyphenols, have a bifidogenic effect in an in vitro fermentation model of the gut microbiota. *Br. J. Nutr.* **2019**, *121*, 549–559. [[CrossRef](#)]
39. Berggren, A.M.; Björck, I.M.E.; Nyman, E.M.G.L.; Eggum, B.O. Short-chain fatty acid content and pH in caecum of rats given various sources of carbohydrates. *J. Sci. Food Agric.* **1993**, *63*, 397–406. [[CrossRef](#)]
40. McIntyre, A.; Young, G.; Taranto, T.; Gibson, P.R.; Ward, P.B. Different fibers have different regional effects on luminal contents of rat colon. *Gastroenterology* **1991**, *101*, 1274–1281. [[CrossRef](#)]
41. Stark, A.; Nyska, A.; Madar, Z. Metabolic and Morphometric Changes in Small and Large Intestine in Rats Fed High-Fiber Diets. *Toxicol. Pathol.* **1996**, *24*, 166–171. [[CrossRef](#)] [[PubMed](#)]
42. Mitsui, R.; Kubo, Y.; Sugiura, Y.; Kuwahara, A.; Karaki, S.-I. Fibre-free diet leads to impairment of neuronally mediated muscle contractile response in rat distal colon. *Neurogastroenterol. Motil.* **2006**, *18*, 1093–1101. [[CrossRef](#)] [[PubMed](#)]
43. Fukumoto, S.; Tatewaki, M.; Yamada, T.; Fujimiya, M.; Mantyh, C.; Voss, M.; Eubanks, S.; Harris, M.; Pappas, T.; Takahashi, T. Short-chain fatty acids stimulate colonic transit via intraluminal 5-HT release in rats. *Am. J. Physiol. Integr. Comp. Physiol.* **2003**, *284*, R1269–R1276. [[CrossRef](#)] [[PubMed](#)]
44. Höckerfelt, U.; Franzén, L.; Norrgård, Ö.; Forsgren, S. Early increase and later decrease in VIP and substance P nerve fiber densities following abdominal radiotherapy: A study on the human colon. *Int. J. Radiat. Biol.* **2002**, *78*, 1045–1053. [[CrossRef](#)]
45. Yano, J.M.; Yu, K.; Donaldson, G.P.; Shastri, G.G.; Ann, P.; Ma, L.; Nagler, C.R.; Ismagilov, R.F.; Mazmanian, S.K.; Hsiao, E.Y. Indigenous Bacteria from the Gut Microbiota Regulate Host Serotonin Biosynthesis. *Cell* **2015**, *161*, 264–276. [[CrossRef](#)]
46. de Vadder, F.; Grasset, E.; Holm, L.M.; Karsenty, G.; Macpherson, A.J.; Olofsson, L.E.; Bäckhed, F. Gut microbiota regulates maturation of the adult enteric nervous system via enteric serotonin networks. *Proc. Natl. Acad. Sci. USA* **2018**, *115*, 6458–6463. [[CrossRef](#)]
47. Otterson, M.F. Effects of radiation upon gastrointestinal motility. *World J. Gastroenterol.* **2007**, *13*, 2684–2692. [[CrossRef](#)]
48. Morris, K.A.; Haboubi, N.Y. Pelvic radiation therapy: Between delight and disaster. *World J. Gastrointest. Surg.* **2015**, *7*, 279–288. [[CrossRef](#)]
49. Vasina, V.; Barbara, G.; Talamonti, L.; Stanghellini, V.; Corinaldesi, R.; Tonini, M.; De Ponti, F.; de Giorgio, R. Enteric neuroplasticity evoked by inflammation. *Auton. Neurosci.* **2006**, *126–127*, 264–272. [[CrossRef](#)]
50. Brierley, S.M.; Jones, R.W.; Gebhart, G.F.; Blackshaw, A. Splanchnic and pelvic mechanosensory afferents signal different qualities of colonic stimuli in mice. *Gastroenterology* **2004**, *127*, 166–178. [[CrossRef](#)]
51. Lynch, A.C.; Antony, A.; Dobbs, B.R.; Frizelle, A.F. Bowel dysfunction following spinal cord injury. *Spinal Cord* **2001**, *39*, 193–203. [[CrossRef](#)] [[PubMed](#)]
52. Ratto, C.; Grillo, E.; Parello, A.; Petrolino, M.; Costamagna, G.; Doglietto, G.B. Sacral Neuromodulation in Treatment of Fecal Incontinence Following Anterior Resection and Chemoradiation for Rectal Cancer. *Dis. Colon Rectum* **2005**, *48*, 1027–1036. [[CrossRef](#)] [[PubMed](#)]
53. Hauer-Jensen, M.; Denham, J.; Andreyev, H.J.N. Radiation enteropathy—pathogenesis, treatment and prevention. *Nat. Rev. Gastroenterol. Hepatol.* **2014**, *11*, 470–479. [[CrossRef](#)]
54. von Moltke, J.; Ji, M.; Liang, H.E.; Locksley, R.M. Tuft-cell-derived IL-25 regulates an intestinal ILC2-epithelial response circuit. *Nature* **2016**, *529*, 221–225. [[CrossRef](#)]

55. Patel, P.; Malipatlolla, D.K.; Devarakonda, S.; Bull, C.; Rascón, A.; Nyman, M.; Stringer, A.; Tremaroli, V.; Steineck, G.; Sjöberg, F. Dietary Oat Bran Reduces Systemic Inflammation in Mice Subjected to Pelvic Irradiation. *Nutrients* **2020**, *12*, 2172. [[CrossRef](#)] [[PubMed](#)]
56. Yahyapour, R.; Motevaseli, E.; Rezaeyan, A.; Abdollahi, H.; Farhood, B.; Cheki, M.; Rezapoor, S.; Shabeeb, D.; Musa, A.E.; Najafi, M.; et al. Reduction–oxidation (redox) system in radiation-induced normal tissue injury: Molecular mechanisms and implications in radiation therapeutics. *Clin. Transl. Oncol.* **2018**, *20*, 975–988. [[CrossRef](#)]
57. Connors, J.; Dawe, N.; Van Limbergen, J. The Role of Succinate in the Regulation of Intestinal Inflammation. *Nutrients* **2018**, *11*, 25. [[CrossRef](#)]
58. Lei, W.; Ren, W.; Ohmoto, M.; Urban, J.F.; Matsumoto, I.; Margolskee, R.F.; Jiang, P. Activation of intestinal tuft cell-expressed *Sucnr1* triggers type 2 immunity in the mouse small intestine. *Proc. Natl. Acad. Sci. USA* **2018**, *115*, 5552–5557. [[CrossRef](#)]
59. Yi, J.; Bergstrom, K.; Fu, J.; Shan, X.; McDaniel, J.M.; McGee, S.; Qu, D.; Houchen, C.W.; Liu, X.; Xia, L. *Dclk1* in tuft cells promotes inflammation-driven epithelial restitution and mitigates chronic colitis. *Cell Death Differ.* **2019**, *26*, 1656–1669. [[CrossRef](#)]
60. Kawashima, R.; Kawamura, Y.I.; Kato, R.; Mizutani, N.; Toyama–Sorimachi, N.; Dohi, T. IL-13 Receptor $\alpha 2$ Promotes Epithelial Cell Regeneration From Radiation–Induced Small Intestinal Injury in Mice. *Gastroenterology* **2006**, *131*, 130–141. [[CrossRef](#)]